Optics Communications 284 (2011) 3264–3268

Contents lists available at ScienceDirect

Optics Communications

journal homepage: www.elsevier.com/locate/optcom

# Characterization of Rayleigh backscattering performance of CS-SSB signal in carrier distributed passive optical network

C.H. Wang [a], C.H. Yeh [b], C.W. Chow [a,*], Y.F. Wu [a], F.Y. Shih [a], S. Chi [a,c]

[a] Department of Photonics and Institute of Electro-Optical Engineering, National Chiao Tung University, Hsinchu 30010, Taiwan
[b] Information and Communications Research Laboratories, Industrial Technology Research Institute, Chutung, Hsinchu 31040, Taiwan
[c] Department of Electro-Optical Engineering, Yuan Ze University, Chung-Li 3003, Taiwan

ARTICLE INFO

*Article history:*
Received 26 March 2010
Received in revised form 24 March 2011
Accepted 24 March 2011
Available online 7 April 2011

*Keywords:*
Passive optical networks (PONs)
Single sideband (SSB)
Rayleigh backscattering (RB)

ABSTRACT

Rayleigh backscattering (RB) is an intrinsic phenomenon when light propagating in fiber and its level is fixed by the fiber type and the network configuration used. Thus, RB noise would be one of the major impairments in a carrier distributed passive optical network (PON). Previously demonstrated carrier suppressed subcarrier-amplitude modulated phase shift keying (CSS-AMPSK) modulation may be useful to effectively mitigate the RB noise. However, this modulation is basically a carrier suppressed double sidebands modulation (CS-DSB) format, in which the same information is carried by the two sidebands with equal magnitude. This is not very power-efficient for PON. Here, we further extend our RB studies by using carrier suppressed single sideband non-return-to-zero (CS-SSB-NRZ) modulation. We experimentally characterize the CS-SSB-NRZ modulation when subjected to both contributions of RB: Carrier-RB and Signal-RB. Then, numerical simulations are performed, and the results are in good match with the experiment. Finally, upstream transmission experiment is performed showing the feasibility of using the CS-SSB-NRZ signal for the carrier distributed PON. The RB performance of the SSB-NRZ signals transmitted at different distances and driven at different radio-frequency (RF) $f_s$ is also investigated.


## 1. Introduction

Due to the ever-increasing popularity of the Internet and the rapid development of the performances of digital electronics and computers, the bandwidth demand by an individual user will keep on increasing in the near future. The most promising technology to provide broadband delivery is the optical access network, such as passive optical network (PON). PON is very cost-effective, since the network is shared by many users. Recently, wavelength division multiplexed (WDM)-PON and long reach (LR) PONs with centrally distributed light sources and colorless reflective optical networking units (RONUs) [1–4] have attracted much attention. However, when using a single optical fiber to reach the RONU, the distributed continuous wave (CW) carrier and upstream signal must share the same path; and the upstream signal will suffer from impairment generated by Rayleigh backscattering (RB) [5,6]. Several methods have been proposed to mitigate the impact of RB in a carrier distributed PON, including using advanced modulation format [7], wavelength shifting [8] and phase-modulation-induced spectral broadening [9,10]. Recently, we have shown that the carrier suppressed subcarrier-amplitude modulated phase shift keying (CSS-AMPSK) modulation can be useful to effectively mitigate the RB noise. However, this modulation is basically a carrier suppressed double sidebands modulation (CS-DSB) format, in which the same information is carried by the two sidebands with equal magnitude. This is not very power-efficient for the power budget sensitive PON, since half of the upstream power will be filtered out (removed) by the head-end offset arrayed waveguide grating (AWG).

Here, we further extend our RB studies by using carrier suppressed single sideband non-return-to-zero (CS-SSB-NRZ) modulation. In this scheme, only a single feeder fiber is required hence additional feeder fiber is not required when compared with ref. [4]. Besides, the upstream signal is only in simple NRZ format; hence, demodulation is not required when compared with ref. [11]. By using CS-SSB-NRZ modulation, spectral overlap between the CW carrier and the upstream signal can be reduced, hence reducing the interferometric beat noise falling within the head-end office (HO) receiver (Rx) bandwidth. We experimentally characterize the CS-SSB-NRZ modulation when subjected to both contributions of RB: Carrier-RB and Signal-RB. Results show that the CS-SSB-NRZ has negative penalty when compared to NRZ. Besides, numerical simulations are performed, and the results are in good agreement with the experiment. Finally, upstream transmission experiment is performed showing the feasibility of using the CS-SSB-NRZ for the LR-PON. Results show that the RB tolerance in our proposed scheme is better than the traditional NRZ scheme. The RB performance of the SSB-NRZ signals transmitted at different distances and driven at different radio-frequency (RF) $f_s$ is also investigated.

* Corresponding author at: Department of Photonics and Institute of Electro-Optical Engineering, National Chiao Tung University, Rm 216A, TKP building, Hsinchu 30010, Taiwan. Tel.: +886 3 5712121x56334.
*E-mail address:* cwchow@faculty.nctu.edu.tw (C.W. Chow).

0030-4018/$ – see front matter © 2011 Elsevier B.V. All rights reserved.
doi:10.1016/j.optcom.2011.03.064

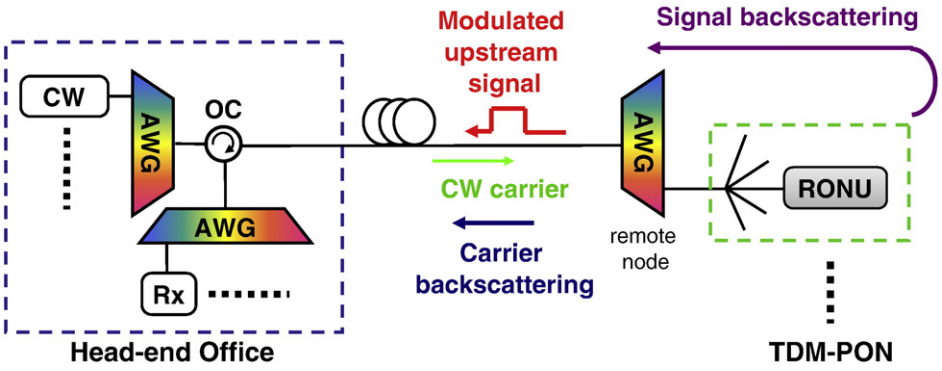


**Fig. 1.** Schematic diagram of RB contributions in a carrier distributed PON.

## 2. Analysis of Rayleigh backscattering

Fig. 1 shows a schematic diagram of a carrier distributed PON. The CW source distributed from the HO and pass through a single drop fiber towards the RONU. The CW source is used as the seeding light for the reflective modulator to generate the upstream signal in the RONU. Due to the intrinsic phenomenon in fiber propagation, there are two contributions to RB which beat with the upstream signals to generate interferometric noise at the Rx inside the HO. The Carrier-RB is generated by the CW carrier sending to the RONU. The Signal-RB is generated by the upstream modulated data signals, remodulated by the RONU and transmitted upwards together with the upstream signals to the Rx at the HO. The two interferometric RB noises are different due to the different optical spectra of the Carrier-RB and the double modulated Signal-RB.

Fig. 2 shows the experimental setups used to investigate the RB tolerance of the CS-SSB-NRZ signal in our proposed scheme, which emulates the impairment of a real PON architecture by producing two interfering signals in the two paths of an interferometer. The left inset of Fig. 2 shows the structure of CS-SSB modulator. In the proof-of-concept experiment, we used a dual-arm Mach–Zehnder modulator (MZM) ($MOD_1$) to produce the CS-SSB optical signal, and we used a single-arm MZM ($MOD_2$) to encode the NRZ data. In implementation, using polarization insensitive semiconductor-based MZM [12] or using a single dual-parallel modulator to generate the CS-SSB-NRZ signal [13] can be practical. The $MOD_1$ was driven in-phase and quadrature-phase by an electrical sinusoidal signal at frequency $f_s = 8$ GHz (with power of +22 dBm) generated by a radio frequency (RF) signal synthesizer. The dual-arm MZM was driven in-phase and quadrature-phase to its two electrodes to cancel the frequency components of one of the

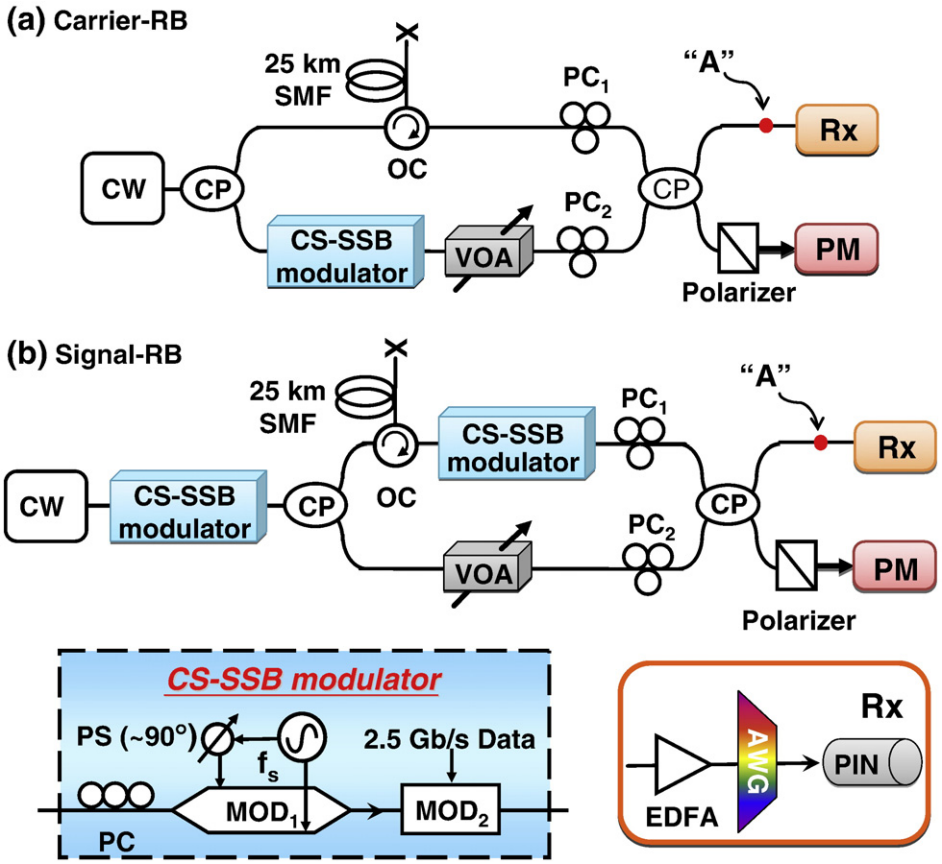


**Fig. 2.** Experimental setup to emulate (a) Carrier-RB and (b) Signal-RB. CW: continuous wave, VOA: variable optical attenuator, CP: optical coupler, PC: polarization controller, PM: power meter. Insets: (left) CS-SSB modulator; MOD1: dual-drive MZM, MOD2: single-drive MZM, PS: phase shifter, (right) Rx architecture; AWG: arrayed waveguide grating.

sidebands. The driving voltage was increased to suppress the center wavelength, i.e. the zero-order of the Bessel function $J_0(\beta)=0$, where the modulation index $\beta=2.4$. Detail description about the SSB generation is reported in [8]. The generated CS-SSB carrier was then encoded by the $MOD_2$ with a 2.5 Gb/s NRZ data at pseudo random binary sequence (PRBS) $2^{31}-1$.

For the analysis of Carrier-RB, as shown in Fig. 2(a), a CW carrier generated by a distributed feedback (DFB) laser with $\lambda=1549.08$ nm and output power of 6 dBm was split into two paths by a 3-dB optical coupler (CP). The Carrier-RB was produced by the CW carrier, which was injected into a 25 km standard single mode fiber (SMF) in the upper arm. The SMF was terminated by an angled connector. The data signal was produced in the lower arm by the CS-SSB modulator. In the lower arm, a variable optical attenuator (VOA) was used to change the signal power; this then changed the power ratios between the optical data signal and Rayleigh noise. We defined this figure of merit as optical signal to Rayleigh noise ratio (OSRNR), which is defined as the ratio of total signal power to the total RB power at the input to the HO (point "A"). To produce the worst case of signal beating, the polarization controllers ($PC_1$ and $PC_2$) were used to make the two signals co-polarized before being combined in the CP. A power meter (PM) was used to monitor the two signals at the output port of the CP. In another port of the CP, Carrier-RB and the upstream signal were both launched into an optically pre-amplified receiver (Rx) as shown in right inset of Fig. 2. The Rx consists of an erbium doped fiber amplifier (EDFA), a tuneable bandpass filter (TBF) (3-dB width of 50 GHz) and a PIN photodiode (bandwidth of 3 GHz). For the Signal-RB analysis, the CW source was firstly modulated by the CS-SSB modulator to emulate the modulated upstream signal in a real PON and then split by a 3-dB CP. The Signal-RB was generated in the upper arm in Fig. 2(b), where the backscattered light from the SMF was re-modulated by another CS-SSB modulator. The Signal-RB from upper arm and the upstream signal from lower arm were combined by a CP and launched into the same Rx as described before.

Figs. 3(a) and (b) shows the Rx sensitivity penalties for a bit error rate (BER) of $10^{-9}$ measured in the experiments. Numerical simulation using VPI Transmission Maker V7.5 were also used to confirm the experimental results. The corresponding eye diagrams at OSRNR of 25 dB were also shown as the insets. The RB performance depends on the interferometric beat noise falling within the Rx bandwidth. For NRZ signal, even relatively low levels of RB can degrade the BER due to the complete spectral overlap between upstream signal and RB components. The CS-SSB-NRZ modulation improves the OSRNR by 6 and 3.5-dB in the Carrier-RB and Signal-RB cases, respectively, at 1-dB power penalty when compare to the conventional NRZ signal. Besides, the result also shows that the Carrier-RB performance of the CS-SSB-NRZ modulation is better than its Signal-RB performance. Numerical simulation results are also given. The performance difference between the simulation and experimental results is due to the fact that the response of the receiver used in simulation was an ideal 3rd order Bessel function; but the receiver used in experiment was not ideal. This accounts for the difference between the simulation and experimental results, particularly at low OSRNR cases. However, the trend of the simulation result agrees with the experimental results.

Fig. 4 shows the experimental optical spectra of the Carrier-RB, upstream data and Signal-RB. The power levels of the three optical spectra are not the same, since their relative powers depend on the OSRNR used. We are interested to observe at the center wavelength, where the spectrum overlap between Carrier-RB and the upstream signal is obviously reduced due to the CS-SSB modulation. Since

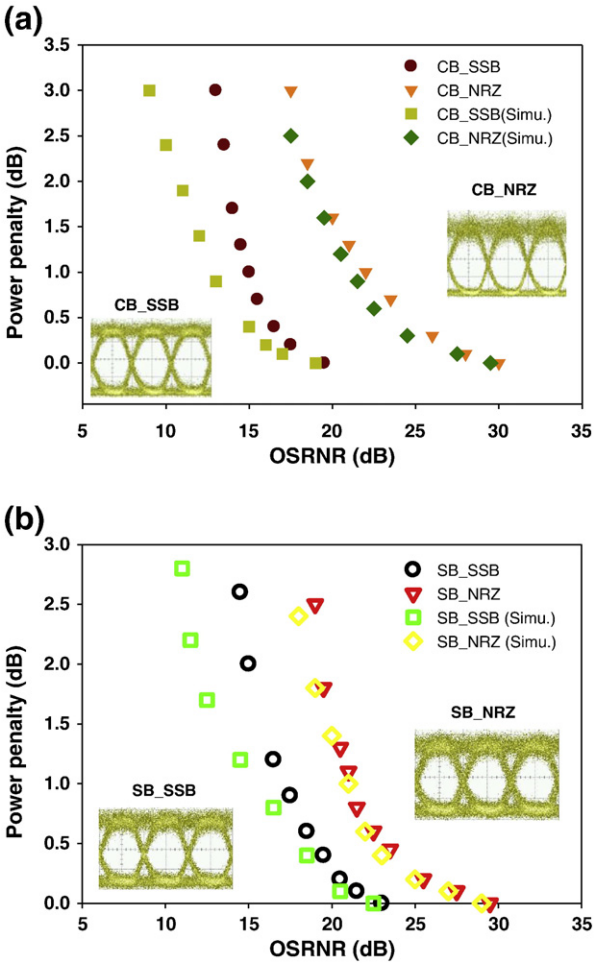


**Fig. 3.** (a) Carrier-RB (CB) (b) Signal-RB (SB) performance at different OSRNRs of CS-SSB-NRZ modulation when compared to conventional NRZ format performed by experiment and simulation. Insets are the corresponding eye diagrams at OSRNR = 25 dB.

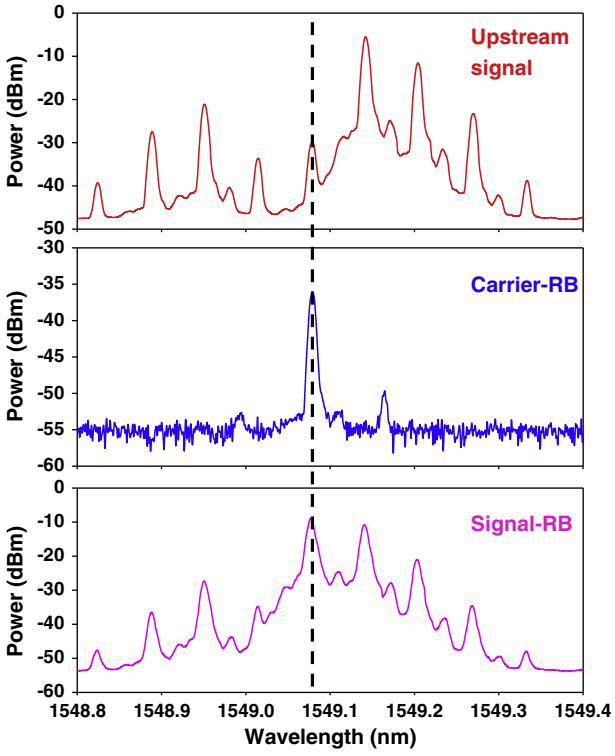


**Fig. 4.** Experimental optical spectra of upstream signal, carrier-RB, and signal-RB.

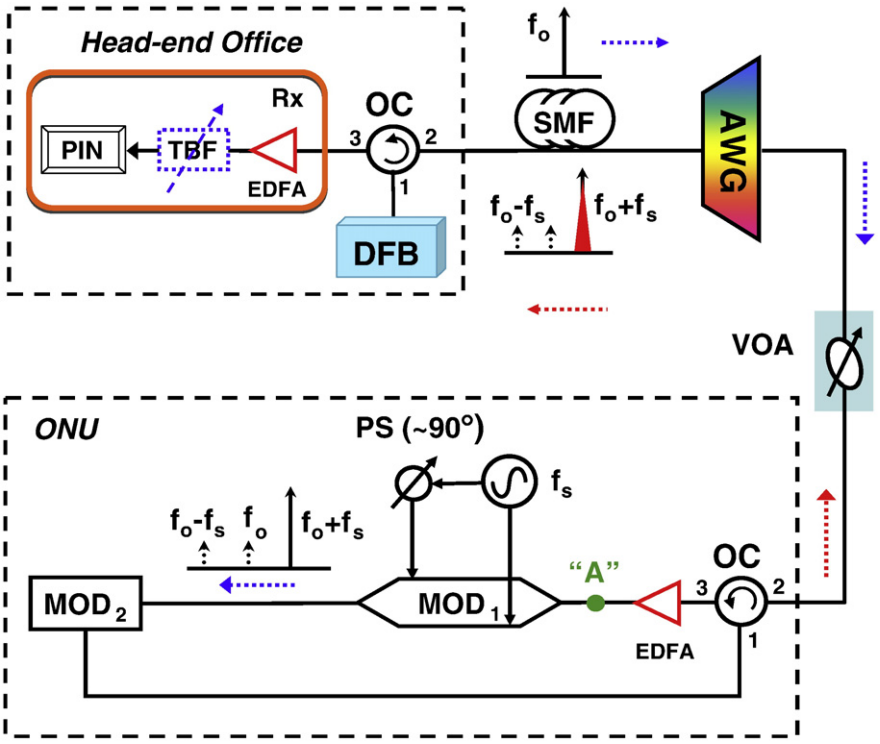


**Fig. 5.** Proposed LR-PON using CS-SSB-NRZ modulation. TBF: tuneable bandpass filter, VOA: variable optical attenuator, OC: optical circulator, PS: phase shifter, $MOD_1$: dual-arm MZM, $MOD_2$: single-arm MZM.

we are measured using an optically pre-amplified Rx, the higher harmonics in the upstream and Signal-RB signals are filtered by the AWG. The interferometric noise was dramatically improved due to the reduced spectrum overlap. The optical spectrum of the Signal-RB is broadened due to the double modulation. We can observe that the center wavelength component rise in the Signal-RB, hence producing higher beat noise than that of the Carrier-RB.

## 3. Transmission performances

Fig. 5 shows the experimental setup of the fully passive LR-PON using CS-SSB-NRZ modulation. A DFB laser set at 1549.8 nm (f0) was used as a CW source. The CW carrier was transmitted through a SMF towards the CS-SSB-NRZ modulator inside the ONU, via an AWG (Gaussian shaped, 3-dB width of 50 GHz). There is no active component between the HO and the ONU, and the LR-PON is fully passive. In the colorless ONU, a loop-back configuration was achieved by an OC. Our proposed SSB-NRZ modulation consisted of a dual-arm MZM ($MOD_1$) and a single-arm MZM ($MOD_2$). The dual-arm MZM was driven in-phase and quadrature-phase by an electrical sinusoidal signal at frequency $f_s$ generated by a RF signal synthesizer. An EDFA (Saturated power = 23 dBm, noise figure = 5 dB) were used in the ONU to compensate the losses of the fiber transmission and the modulators. The generated CS-SSB-NRZ carrier was then encoded by the MOD2 with a 2.5 Gb/s NRZ data at PRBS $2^{31}$-1. The uplink signal was then sent back to the HO through the same SMF. An optically pre-amplified Rx at the HO, consisted of an EDFA, a TBF (3-dB width of 50 GHz) and a PIN photodiode (bandwidth of 3 GHz), was used to detect the uplink signal. No dispersion compensation was used in the experiment.

Fig. 6 shows the optical spectra measured by an optical spectrum analyzer with resolution of 0.01 nm at transmission of 30 km SMF. Dashed line is the distributed CW carrier at wavelength of 1548.79 nm measured at the input of the dual-arm MZM (point "A"). Solid line is the CS-SSB-NRZ modulated uplink signal RF driven at $f_s$ = 8 GHz measured at the Rx at the HO. The power ratios between the upper sideband and the lower sideband and the center wavelength are ~25 dB. Since the RB tolerance depends on the interferometric beat noise falling within the Rx bandwidth, the RB tolerance of the CS-SSB-NRZ modulation can be improved due to the reduced spectral overlap between the uplink signal and the CW carrier.

Fig. 7 shows the bit error rate (BER) measurements of uplink CS-SSB-NRZ with $f_s$ = 8 GHz (case 1) and the NRZ signals (case 2, without the SSB modulator $MOD_1$) at back-to-back (B2B) and transmission of 30 km, 90 km, respectively, without dispersion compensation. The corresponding eye diagrams are shown in the insets. The results show that the power penalties between the NRZ and the CS-SSB-NRZ signals increased when the transmission distance increased. We observed 3 dB power penalties improvement at the transmission of 30 km. For LR transmission (90 km), an error-floor appears for the NRZ case while error-free operation can still be achieved in CS-SSB-NRZ case, showing the proposed scheme can effectively mitigate RB noise in carrier-distributed networks, particularly in LR-PON.

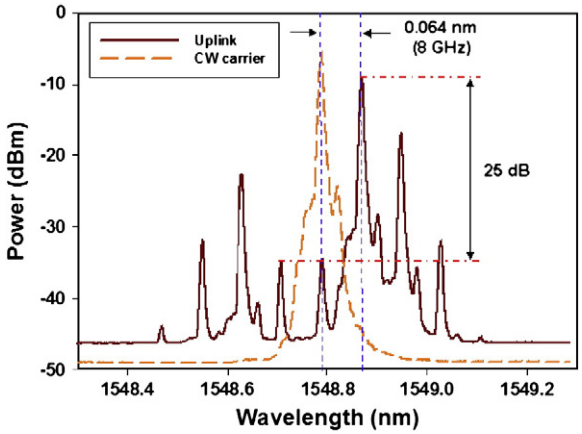


**Fig. 6.** Optical spectra. Solid line is for uplink CS-SSB-NRZ signal. Dashed line is for CW carrier.

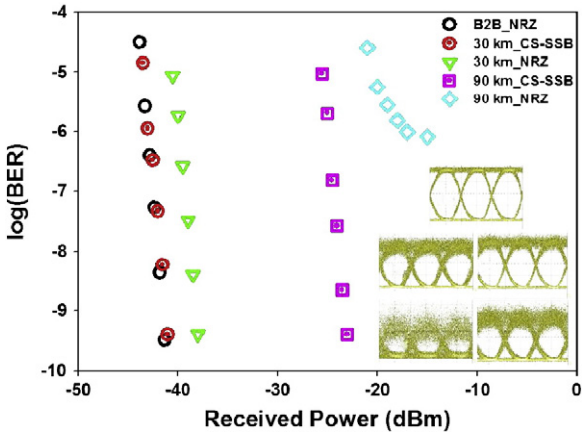


**Fig. 7.** BER measurements of the upstream traditional NRZ (case 1) and CS-SSB-NRZ (case 2) signals. Insets: eye diagrams of (a) case 1 at back-to-back (B2B) transmission, (b) case 1 after 30 km transmission, (c) case 1 after 90 km transmission, (d) case 2 after 30 km transmission, (e) case 2 after 90 km transmission.

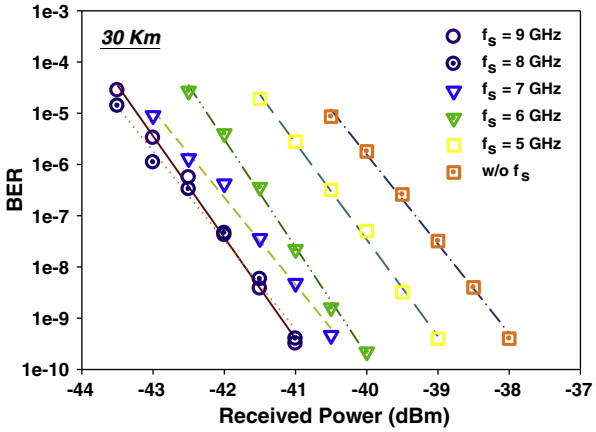


**Fig. 8.** BER performances of different RF frequency $f_s$ versus Rx received power at transmission of 30 km.

Fig. 8 shows the BER performances of the CS-SSB-NRZ signals at different fs versus Rx received powers (30 km transmission case). We also tested at $f_s = 9$ GHz, and its performance is nearly the same as that of $f_s = 8$ GHz. The result shows that the RB performance of the CS-SSB-NRZ improves when $f_s$ increases (due to the reduced spectral overlap between the CW carrier and the uplink signal), and saturates at about $f_s = 8$ GHz. This is limited by the bandwidth of the dual-arm MZM (10 GHz). We believe that the data rate and the BER performance can be further improved if larger bandwidth modulator is available.

## 4. Conclusion

RB is identified as one of the most critical impairments in a carrier distributed PON. Previously we proposed and demonstrated that using CSS-AMPSK modulation may be useful to mitigate the RB noise. However, this modulation is basically a CS-DSB format, in which half of the power is wasted in one of the sideband. This is not very power-efficient for PON. Here, we further extended our RB studies by using CS-SSB-NRZ modulation. We experimentally characterized the CS-SSB-NRZ modulation when subjected to both contributions of RB: Carrier-RB and Signal-RB. Results showed that the CS-SSB-NRZ modulation had 6 dB and 3.5 dB OSRNR improvement in Carrier-RB and Signal-RB respectively over conventional NRZ signal. Numerical simulations were performed with good match. Finally, an upstream transmission experiment was performed using CS-SSB-NRZ modulation. We observed 3 dB power penalties improvement after 30 km of SMF transmission. For LR transmission (90 km), an error-floor appeared at the conventional NRZ case while error-free operation can still be achieved in CS-SSB-NRZ signal, showing the proposed scheme can effectively mitigate RB noise in carrier-distributed PON. The RB performance of the SSB-NRZ signals transmitted at different distances and driven at different radio-frequency (RF) $f_s$ is also investigated.

## Acknowledgement

This work was supported by the National Science Council, Taiwan, under Contracts NSC 98-2221-E-009-017-MY3 and 97-2221-E-009-038-MY3.

## References

[1] L.Y. Chan, C.K. Chan, D.T.K. Tong, F. Tong, L.K. Chen, Upstream traffic transmitter using injection-locked Fabry-Perot laser diode as modulator for WDM access networks, Electron. Lett. 38 (2002) 43–45.
[2] W. Hung, C.K. Chan, L.K. Chen, F. Tong, An optical network unit for WDM access networks with downstream DPSK and upstream remodulated OOK data using injection-locked FP laser, IEEE Photon. Technol. Lett. 15 (2003) 1476–1478.
[3] C.W. Chow, Wavelength remodulation using DPSK down-and-upstream with high extinction ratio for 10-Gb/s DWDM-passive optical networks, IEEE Photon. Technol. Lett. 20 (2008) 12–14.
[4] G. Talli, C.W. Chow, E.K. MacHale, P.D. Townsend, Long reach hybrid DWDM-TDM PON with high split ratio employing centralized light source, J. Opt. Networking 6 (2007) 765–776.
[5] S.-K. Liaw, S.-L. Tzeng, Y.-J. Hung, Power penalty induced by Rayleigh backscattering in a bidirectional wavelength-reuse lightwave system, Proc. CLEO, 2001, CThL54, 2001.
[6] G. Talli, D. Cotter, P.D. Townsend, Rayleigh backscattering impairments in access networks with centralised light source, Electron. Lett. 42 (2006) 877–878.
[7] Z. Li, Y. Dong, Y. Wang, C. Lu, A novel PSK—Manchester modulation format in 10-Gb/s passive optical network system with high tolerance to beat interference noise, IEEE Photon. Technol. Lett. 17 (2005) 1118–1120.
[8] J. Prat, M. Omella, V. Polo, Wavelength shifting for colorless ONUs in single-fiber WDM-PONs, Proc. OFC (2007), Anaheim, CA, OFE1, 2007.
[9] C.W. Chow, G. Talli, P.D. Townsend, Rayleigh noise reduction in 10-Gb/s DWDM-PONs by wavelength detuning and phase-modulation-induced spectral broadening, IEEE Photon. Technol. Lett. 19 (2007) 423–425.
[10] C.W. Chow, G. Talli, A.D. Ellis, P.D. Townsend, Rayleigh noise mitigation in DWDM LR-PONs using carrier suppressed subcarrier-amplitude modulated phase shift keying, Opt. Express 16 (2008) 1860–1866.
[11] J. Xu, L.K. Chen, C.K. Chan, Phase-modulation-based loopback scheme for Rayleigh noise suppression in 10-Gb/s carrier-distributed WDM-PONs, IEEE Photon. Technol. Lett. 22 (2010) 1343–1345.
[12] O. Leclerc, P. Brindel, D. Rouvillain, E. Pincemin, B. Dany, E. Desurvire, C. Duchet, E. Boucherez, S. Bouchoule, 40 Gbit/s polarization-insensitive and wavelength-independent InP Mach-Zehnder modulator for all-optical regeneration, Electron. Lett. 35 (1999) 730–732.
[13] S. Shimotsu, S. Oikawa, T. Saitou, N. Mitsugi, K. Kubodera, T. Kawanishi, M. Izutsu, Single side-band modulation performance of a $LiNbO_3$ integrated modulator consisting of four-phase modulator waveguides, IEEE Photon. Technol. Lett. 13 (2001) 364–366.